Biochimica et Biophysica Acta, 601 (1980) 22—33

BBA 78891

^{2}H- AND ^{31}P-NMR STUDIES OF CHOLESTERYL PALMITATE IN SPHINGOMYELIN DISPERSIONS

ALEX L. MACKAY [a,*], STEPHEN R. WASSALL [b], MARKO I. VALIC [a], HEINER GORRISSEN [b] and ROBERT J. CUSHLEY [b,*]

[a] *Department of Physics, University of British Columbia, Vancouver, British Columbia, V6T 1W5, and* [b] *Department of Chemistry, Simon Fraser University, Burnaby, British Columbia, V5A 1S6 (Canada)*

(Received February 29th, 1980)

Key words: Cholesterol ester incorporation; Phase behavior; Order parameter; Cholesterol; Atherosclerosis; NMR

Summary

Dispersions (50 wt% in water) of sphingomyelin/cholesteryl palmitate (95 : 5 mol%) have been studied by ^{2}H- and ^{31}P-NMR spectroscopy between 25 and 60°C. The deuterated esters, cholesteryl palmitate-d_{31} and cholesteryl palmitate-16, 16, 16-d_3, were used for ^{2}H-NMR studies. Of the 5 mol% cholesteryl palmitate added, 1.5 mol% was found to incorporate in the sphingomyelin and this amount remained constant throughout the temperature range studied. The remainder of the cholesteryl palmitate was present as regions of solid. At temperatures above the gel-to-liquid crystalline phase transition of sphingomyelin the NMR spectra indicate that a fraction of the cholesteryl palmitate and sphingomyelin is undergoing rapid isotropic motions. This fraction, which increases with increasing temperature above the phase transition, is probably composed of small bilayer structures.

When 50 mol% cholesterol (relative to sphingomyelin) was added to the sphingomyelin/cholesteryl palmitate dispersion, the isotropic component in the NMR spectra was no longer present, the gel-to-liquid crystalline phase transition was removed, and the incorporation of ester in the membrane decreased by more than an order of magnitude.

Introduction

Fatty acid esters of cholesterol are known to build up rapidly during the progression of atherosclerosis. The first clinical signs of the disease — fatty

* To whom reprint requests should be addressed.

streaks in the human aorta — are composed of up to 95% cholesteryl ester [1]. As well, even before morphological changes occur, certain areas of the aortic intima are predisposed to development of atherosclerotic lesions. Such areas have been associated with areas of increased cholesteryl ester content and increased permeability [2]. Since an earlier study [3] showed that cholesteryl palmitate increased the permeability of model membranes, we have initiated studies on the structural organization of model membranes containing cholesteryl esters. Recently, Valic et al. [4] reported the observation of ^{2}H-NMR spectra of cholesteryl palmitate-d_{31} and cholesteryl palmitate-16, 16, 16-d_3 in egg phosphatidylcholine lamellar systems and found that only about 0.2 mol% of cholesteryl palmitate dissolved in the lipid.

Since the phospholipid composition of human aorta shows an increase in sphingomyelin content from 35 to 63% as atherosclerotic disease progresses (and a concurrent drop in phosphatidylcholine from 43 to 23%) [5], we decided to investigate the sphingomyelin/cholesteryl ester/water system. We present here the results of a ^{2}H- and ^{31}P-NMR study of lipid dispersions composed of 50 wt% sphingomyelin/cholesteryl palmitate (95 : 5 mol%)/50 wt% water. The esters studied were cholesteryl palmitate-d_{31} and cholesteryl palmitate-16, 16, 16-d_3.

^{2}H-NMR was chosen since ^{2}H is a non-perturbing probe of local orientational order and mobility of lipid bilayers [6,7]. The usefulness of the ^{2}H-NMR technique has been enhanced recently by introduction of the quadrupolar echo technique [8] to give essentially distortion-free ^{2}H-NMR spectra. The use of ^{31}P-NMR allows us to monitor the phase of the sphingomyelin [9]. This was necessary in light of recent ^{31}P-NMR evidence indicating the presence of appreciable amounts of non-lamellar phase structures for sphingomyelin in aqueous dispersions [10—12].

Materials and Methods

Bovine brain sphingomyelin was either purchased from Sigma Chemical Co. or prepared as described below. Cholesterol was obtained from Fisher Scientific Co. and recrystallized from benzene before being used. Deuterium-depleted water was purchased from Aldrich Chemical Co. Palmitic-d_{31} acid was obtained from Merck, Sharp and Dohme, Canada and palmitic-16, 16, 16-d_3 acid obtained from Serdary Research Laboratories, London, Ontario, Canada. Cholesteryl palmitate was obtained from Sigma Chemical Co., while cholesteryl palmitate-16, 16, 16-d_3 and cholesteryl palmitate-d_{31} were synthesized using a published procedure [13].

In a typical sphingomyelin extraction, 500 g of fresh bovine brain were used, and crude sphingolipids were obtained essentially as described by Carter et al. [14]. The dry sphingolipids were dispersed in 100 ml of glacial acetic acid at room temperature and filtered in order to remove cerebrosides. The filtrate, which contains the sphingomyelin, was brought to dryness under vacuum and was then subjected to an alkaline hydrolysis as described by Sweeley [15] in order to remove glycerophospholipids. The crude sphingomyelin was then purified on a silica gel column. Impurities were eluted from the column with chloroform/methanol (1 : 1 and 1 : 4), while pure sphingo-

myelin was eluted with chloroform/methanol (1 : 9). Typically, the yield was approx. 1.5 g.

Fatty acid methyl esters of sphingomyelin were prepared by dissolving 100 mg of the lipid in 2 ml of 3 M methanolic HCl and 2 ml of 2,3-dimethoxypropane, and then heating the solution in a stoppered tube under N_2 for 3 h at 65—70°C. The methyl esters were extracted from the mixture with petroleum ether and analyzed on a Varian Series 2100 gas chromatograph equipped with a flame ionization detector, using a 23 m × 0.27 mm inner diameter capillary column coated with Silar 10C. The instrument was programmed from 150 to 215°C, at a rate of 2°C/min. Mass spectra were run on an HP 5985 GC/MS system.

Differential scanning calorimetry (DSC) experiments were performed on a Perkin-Elmer DSC-1B calorimeter using a scanning rate of 5°C/min.

The ^{2}H-NMR measurements were carried out at 37.2 MHz with a Bruker SXP 4-100 NMR spectrometer and a Nalorac superconducting magnet. In the Spin-Tech Electronics probe head the sample chamber was enclosed by an oven in which the temperature could be regulated to ±0.1°C with a Bruker BST 100-700 temperature controller. An Intel 8080A microprocessor-based computer interfaced to a Nicolet 1090 AR digital oscilloscope was used to collect the NMR signals, and Fourier transforms were calculated on a Nicolet BNC-12 mini-computer.

To eliminate spectral distortion due to the receiver recovery time, data acquisition was initiated at the peak of the quadrupolar echo generated by a

$$\left.\frac{\pi}{2}\right|_{0^\circ} - \tau_1 - \left.\frac{\pi}{2}\right|_{90^\circ}$$

pulse sequence [8]. For most of our measurements a value of $\tau_1 = 80$ μs was used and the sequence was repeated after a time τ_r (usually 1.5 s). For every second pulse sequence, the phase of the first pulse was changed by 180° and alternate scans were subtracted from the accumulative data memory, resulting in the cancellation of coherent receiver and pulse noise.

A Varian XL-100-15 NMR spectrometer, interfaced to a Nicolet 1080 computer and operating in the pulse Fourier transform mode, was employed in the ^{31}P-NMR experiments. The free induction decays were recorded at an operating frequency of 40.5 MHz, using an external ^{19}F field frequency lock, and in the presence of ^{1}H noise decoupling which usually covered a 2 kHz bandwidth. The ^{31}P pulse length was 20 μs, corresponding to a flip angle of approx. 30°. The sweep width was 10 kHz, and 4K data sets were collected with external H_3PO_4 (85%) as a reference. Temperature control to within ±1°C was accomplished using a gas flow system.

Throughout the ^{31}P-NMR experiments the output (10 W) of the decoupler was applied to the transmitter coils which are closer to the sample than the coils normally used for decoupling. The transmitter pulses (^{31}P) were applied to the coils to which the decoupler is normally connected. It is estimated that an increase in decoupling power at the sample of greater than a factor of 2 compared to the conventional probe arrangement was achieved and an improvement in the resolution of the ^{1}H noise-decoupled ^{31}P spectra was obtained.

NMR samples were prepared by dissolving sphingomyelin, cholesteryl ester

and, where appropriate, cholesterol in chloroform/methanol (3 : 1). The solvent was then removed by evaporation under a stream of N_2 and subsequent overnight pumping under high vacuum. Lipid dispersions were prepared by adding an equal weight of water (for ^{31}P-NMR) or deuterium-depleted water (for ^{2}H-NMR) to the dry lipid mixture and vigorously shaking with a vortex mixer at approx. 50°C until the sample was homogeneous.

Results

A recent report [16] indicates that there are significant variations in fatty acid composition of bovine brain sphingomyelin obtained from different sources. Therefore, the sphingomyelin obtained commercially and that isolated in the present study were analyzed for fatty acid composition. The results of a gas chromatography-mass spectral analysis of the two sphingomyelins are reported in Table I. The Table indicates that the fatty acid composition of the two sphingomyelins are essentially the same, and they were used interchangeably throughout the study.

Calorimetric studies on a 50 wt% sphingomyelin/cholesteryl palmitate (95 : 5 mol%)/50 wt% water dispersion were performed to check whether the addition of 5 mol% cholesteryl palmitate has a significant effect on the thermal behavior. The DSC curves for this sample indicated a broad transition region with peaks at 34 and 40°C, which is unchanged from the curve for sphingomyelin alone and in reasonable agreement with published DSC curves of pure sphingomyelin mixtures [17,18], so we conclude that the effect of the dissolved ester on the sphingomyelin phase transition is minimal. Addition of 50 mol% cholesterol (based on sphingomyelin) completely removed the gel-to-liquid crystalline phase transition between 20 and 60°C, as previously reported for a cholesterol/*N*-palmitoylsphingomyelin aqueous dispersion [19].

^{2}H-NMR

Fig. 1 illustrates the temperature dependence of the ^{2}H-NMR spectra for a

TABLE I

FATTY ACID COMPOSITION OF SPHINGOMYELIN

Fatty acid	Bovine brain sphingomyelin (%)	
	Sigma	Prepared in this laboratory
16 : 0	6.0	2.9
18 : 0	38.2	46.6
20 : 0	1.9	1.3
22 : 0	4.0	5.0
23 : 0	2.5	3.4
24 : 0	6.9	10.5
24 : 1 + 23 : 3 *	32.8	27.3
23 : 3	3.9	2.9
24 : 2	3.8	0.1

* These two compounds are not resolved on our gas-liquid chromatography column.

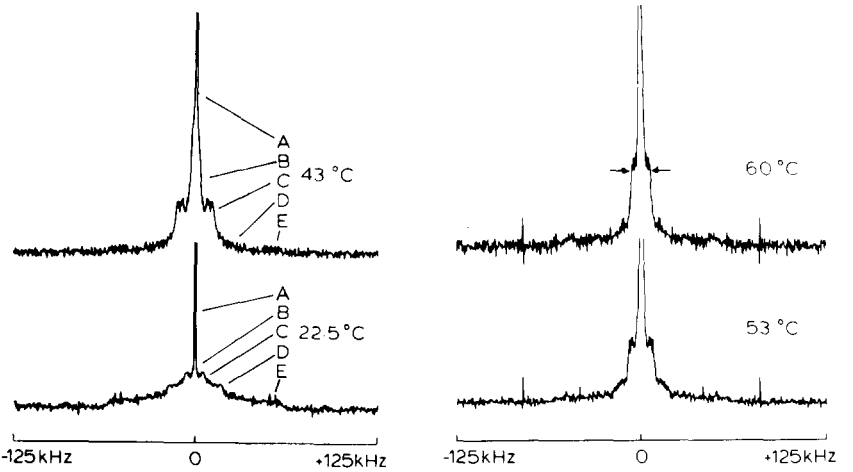

Fig. 1. ^{2}H-NMR spectra for the dispersion 50 wt% sphingomyelin/cholesteryl palmitate-d_{31} (95 : 5 mol%)/50 wt% H_2O. The features A—E are explained in the text. The arrows indicate where the signal width was measured for Fig. 2. The Fourier transform spectra were obtained from approx. 8000 transients collected in 4K data points with a spectral width of 500 kHz and a pulse width = 5 μs.

lipid dispersion made up of 50 wt% sphingomyelin/cholesteryl palmitate-d_{31} (95 : 5 mol%)/50 wt% deuterium-depleted water. The complex spectra presented are interpreted as a superposition of spectra from cholesteryl palmitate-d_{31} in three different environments plus ^{2}HOH. The main features of the superposed spectra are labelled A—E in Fig. 1. Features D and E, seen as broad shoulders in the 43°C spectrum, have splittings of 37 and 126 kHz, respectively, identical to those found for C^2H_3 and $(C^2H_2)_n$ in the ^{2}H-NMR spectrum of solid cholesteryl palmitate-d_{31} [4] and we ascribe D and E to regions of solid cholesteryl palmitate within the dispersion. D has reduced intensity because the repetition time was short (τ_r = 1.5 s) compared to the T_1 value of $(C^2H_2)_n$ (T_1 = 11.4 s) for solid cholesteryl palmitate [4]. Feature C is attributed to $(C^2H_2)_n$ and C^2H_3 on cholesteryl palmitate molecules dissolved in the sphingomyelin bilayers. In spectra acquired at temperatures greater than 40°C, an additional narrow signal (B) was observed which becomes more intense at higher temperatures and which we attribute to dissolved cholesteryl palmitate undergoing isotropic motions. Finally, there is a small central peak (A) which arises from residual ^{2}HOH and is present in all spectra.

The most distinctive feature of the cholesteryl palmitate-d_{31} spectra is the large temperature variation in the shape of the C signal. A plot of signal width of C (as indicated in Fig. 1) vs. temperature is given in Fig. 2. The signal width is related to the distribution of segmental C-^{2}H splitting and, hence, the organization of the ester acyl chain and it varies from 29 to 12 kHz between 40 and 60°C (at temperatures less than 40°C, the signal was so broad that it could not be separated from the solid ester signal). For comparison, we have also plotted, in Fig. 2, the width of the ^{2}H quadrupolar spectrum from a dispersion of 50 wt% dipalmitoyl-d_{62}-phosphatidylcholine/50 wt% H_2O [20].

The ^{2}H-NMR spectra from cholesteryl palmitate-d_{31} in sphingomyelin contain several overlapping components and the T_1 value of the solid methylene

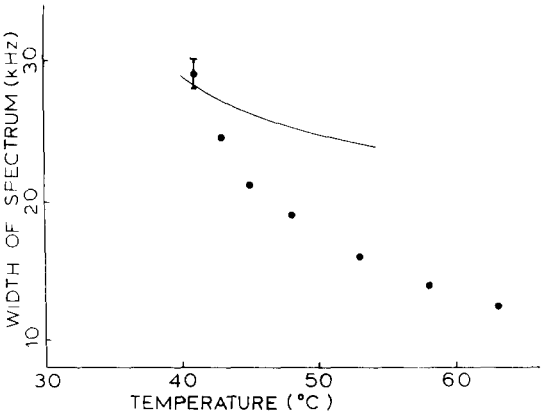

Fig. 2. Plot of the width of the ^{2}H-NMR signal from cholesteryl palmitate-d_{31} incorporated into sphingomyelin vs. temperature. The continuous line represents the width of the ^{2}H-NMR spectra of a 50 wt% dipalmitoyl-d_{62}-phosphatidylcholine/50 wt% H_2O dispersion taken from Ref. 8.

signal is very long. Therefore, it would be difficult to determine the amount of incorporation of ester in the phospholipid bilayer from our cholesteryl palmitate-d_{31} data. We have repeated the measurements using cholesteryl palmitate-16, 16, 16-d_3 in sphingomyelin dispersions since the resulting ^{2}H spectra are simpler and $T_1 = 0.24$ s for solid cholesteryl palmitate-16, 16, 16-d_3 [4]. Spectra for four representative temperatures are shown in Fig. 3. These spectra have four components (A—D) and we assign D to solid cholesteryl palmitate, C to cholesteryl palmitate dissolved in sphingomyelin bilayers, B to dissolved cholesteryl palmitate undergoing rapid, isotropic reorientation and A to ^{2}HOH. We shall elaborate on our assignment of B in a later section.

From the C component of the spectra in Fig. 3, we can measure the C^2H_3 quadrupolar splitting and calculate the C-^{2}H order parameter for the methyl deuterons of cholesteryl palmitate dissolved in sphingomyelin. The segmental

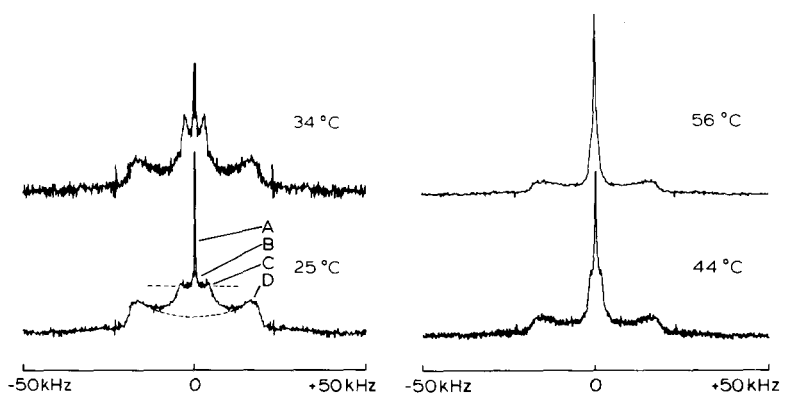

Fig. 3. ^{2}H-NMR spectra for the dispersion 50 wt% sphingomyelin/cholesteryl palmitate-16, 16, 16-d_3 (95 : 5 mol%)/50 wt% H_2O. The features A—D are described in the text. The separation of the signals B from C and C from D was made at the interface indicated by the dashed lines. The Fourier transform spectra were obtained from approx. 8000 transients collected in 4K data points with a spectral width of 200 kHz and a pulse width = 5 μs.

order parameter for the C-^{2}H bond, S_{C^2H}, is related to the quadrupolar splitting by the relationship:

$$\Delta\nu_Q = \frac{3}{4} \cdot \frac{e^2qQ}{h} |S_{C^2H}| \tag{1}$$

where (e^2qQ/h) is the static quadrupolar coupling constant (168 kHz for a deuterium on a methyl or methylene group [21,22]), and

$$S_{C^2H} = \left\langle \frac{3\cos^2\gamma - 1}{2} \right\rangle \tag{2}$$

where γ is the angle between the C-^{2}H bond and the axis of symmetry for reorientational motions of this bond, and the angular brackets represent an average over all conformations of the molecule. A plot of the C^2H_3 order parameter vs. temperature is presented in Fig. 4. The order parameter curve has a change in slope at approx. 39°C which corresponds to a temperature within the gel-to-liquid crystalline phase transition of the sphingomyelin. In Fig. 4 we have also plotted, for comparison, the temperature dependence of the C-^{2}H order parameter of the terminal methyl groups in a 50 wt% dipalmitoyl-d_{62}-phosphatidylcholine/50 wt% water dispersion [21].

The percent of dissolved ester,

$$\% \text{ dissolved ester} = \frac{\text{Area(B + C)}}{\text{Area(B + C + D)}} \times 100\% \tag{3}$$

where the B, C and D components are taken from Fig. 3, is plotted vs. temperature in Fig. 5. If the spectral areas are to be treated as proportional to the number of molecules, the recovery time between pulse sequences, τ_r, should be much longer than T_1 for any of the deuterons contributing to the signal and the τ_1 values used in the quadrupolar echo sequence should be much less than the echo decay times (T_{2e}) for the deuterons. Our experiments satisfied the first criterion, but we found that the T_{2e} value for cholesteryl palmitate-

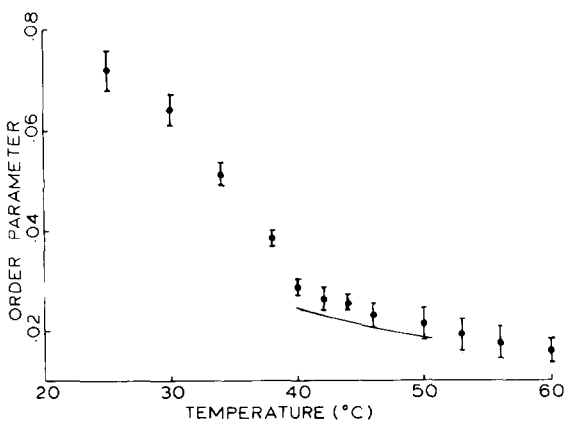

Fig. 4. Plot of the C-^{2}H order parameter for the C^2H_3 group of cholesteryl palmitate-16, 16, 16-d_3 in sphingomyelin vs. temperature. For comparison, the order parameter for the methyl group in the dispersion 50 wt% dipalmitoyl-d_{62}-phosphatidylcholine/50 wt% H_2O [8] is shown by the continuous line.

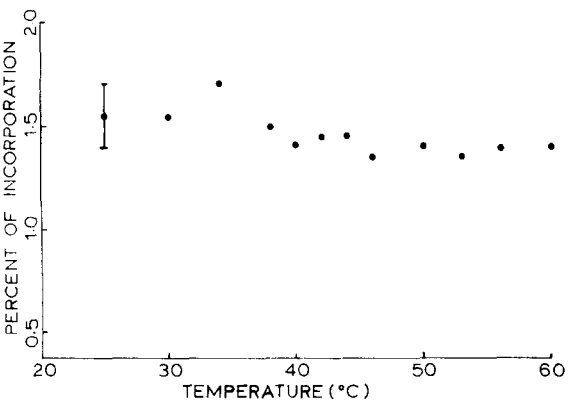

Fig. 5. Plot of percent incorporation of cholesteryl palmitate in sphingomyelin vs. temperature.

16, 16, 16-d_3 in sphingomyelin varied from about 200 μs at 25°C to more than 1 ms at 50°C and was 400 μs for the solid cholesteryl palmitate-16, 16, 16-d_3. The measured peak areas, $A(2\tau_1)$, have been extrapolated to those which would have been obtained at $\tau_1 = 0$ using the relationship:

$$A(2\tau_1) = A(0) \exp(-2\tau_1/T_{2e}) \tag{4}$$

The areas, $A(0)$, are directly proportional to the number of deuterons contributing to each spectral component.

When the percent of the isotropic component of cholesteryl palmitate dissolved in the membrane is calculated, namely,

$$\% \text{ isotropic component} = \frac{\text{Area(B)}}{\text{Area(B + C)}} \times 100\% \tag{5}$$

then a plot of percent isotropic component vs. temperature, (Fig. 6) reveals that above the phase transition temperature for sphingomyelin the isotropic component increases with increasing temperature. The estimated error in this measurement is ±30%, mainly due to the overlap of the B and C spectral components.

In addition, we carried out ^{2}H-NMR of a 50 wt% cholesterol/sphingomyelin/cholesteryl palmitate-d_{31} (47.5 : 47.5 : 5 mol%)/50 wt% water dispersion at four temperatures between 25 and 55°C and found less than 0.1 mol% incorporation of cholesteryl palmitate into the membrane in this temperature range, an amount less than a tenth of that found for cholesteryl palmitate in pure sphingomyelin.

^{31}P-NMR

Proton noise-decoupled ^{31}P-NMR spectra for a 50 wt% bovine brain sphingomyelin/cholesteryl palmitate (95 : 5 mol%)/50 wt% water sample were recorded as a function of temperature in the range of 20—80°C, and representative spectra at three temperatures are shown in Fig. 7. The spectrum at 55°C (Fig. 7) is clearly not the simple powder pattern characteristic of phospholipids in the lamellar phase [9]. Instead, it is interpreted as the superposition of a lamellar phase powder pattern and a narrow line, chemically

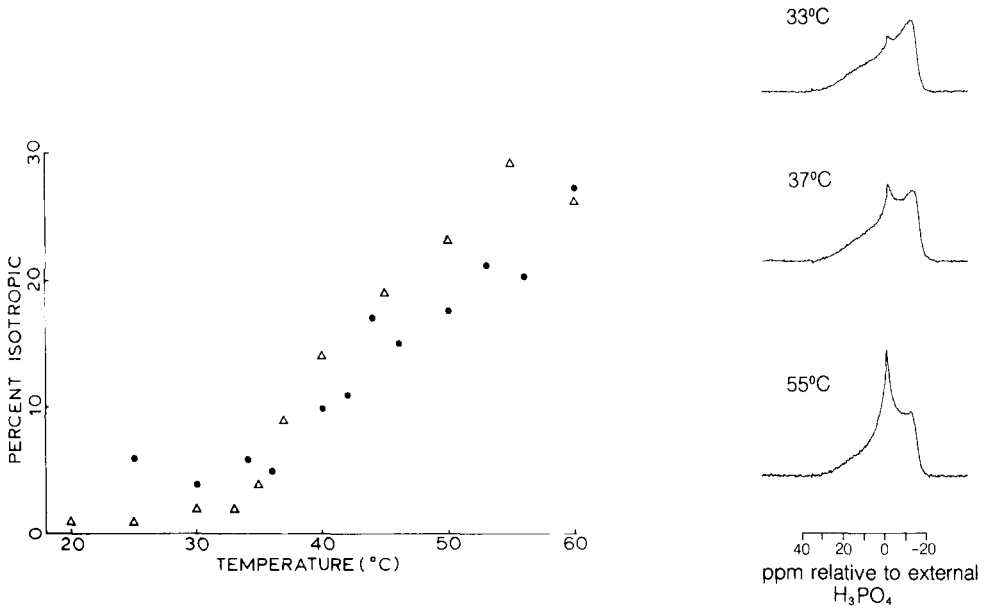

Fig. 6. Plot of percent isotropic component of cholesteryl palmitate dissolved in sphingomyelin as determined by ^{2}H-NMR (•), and the percent of sphingomyelin in the isotropic signal of the ^{31}P-NMR spectra (△), vs. temperature.

Fig. 7. Proton noise-decoupled ^{31}P-NMR spectra for the dispersion 50 wt% sphingomyelin/cholesteryl palmitate (95 : 5 mol%)/50 wt% H_2O. Fourier transform spectra were obtained from approx. 2000 transients collected at a repetition rate of 2 s and a line broadening parameter = 5 Hz.

shifted 1 ppm upfield from H_3PO_4, due to sphingomyelin undergoing isotropic motions ($\tau_c << 1 \cdot 10^{-4}$ s). A similar interpretation may be given to the spectra obtained at all the other temperatures, although the relative intensity of the isotropic signal at temperatures below the gel-to-liquid crystalline transition is rather small, as illustrated by Fig. 7. The chemical shift anisotropy measured for the powder pattern component throughout the temperature range investigated is $\Delta\sigma_{eff}$ = 40—45 ppm, and the estimated width at half-height of the isotropic component over the temperature region 40—80° C, when it makes a significant contribution to the total intensity, is constant to within experimental error at $\Delta\nu_{1/2}$ = 170 ± 30 Hz.

The relative intensity of the isotropic signal is, as mentioned above and indicated by the spectra presented in Fig. 7, dependent upon temperature and the variation with temperature to 60° C is depicted graphically in Fig. 6. The graph shows that the amount of isotropic signal contributing to the spectra is very small, and approximately constant at 1—2%, below the phase transition, and then increases continuously with rising temperature once the transition is reached. This behavior is similar to the dependence on temperature followed by the proportion of incorporated cholesteryl palmitate-16, 16, 16-d_3, giving rise to an isotropic ^{2}H line. The ^{31}P relative intensities were estimated from a comparison of the areas under the narrow and broad spectral components, and are very approximate (±30%). This is due to the difficulty in making a

precise separation of the two contributions to the composite ^{31}P lineshape, and the values estimated for the isotropic component may well be conservative.

Proton noise-decoupled ^{31}P-NMR spectra were also determined for a sphingomyelin/water dispersion and for a dispersion composed of 50 wt% sphingomyelin/cholesterol/cholesteryl palmitate (47.5 : 47.5 : 5 mol%)/50 wt% water. In the former case, the spectra are essentially the same as in the presence of the ester. However, no isotropic signal was present in the spectra in the latter case. Throughout the temperature range 25—60° C only the conventional lamellar phase powder pattern was produced following the inclusion of cholesterol. This effect of cholesterol had been found previously for pure sphingomyelin/H_2O dispersions [11].

Discussion

The most significant finding of the present study, as illustrated by Fig. 5, is the fact that the amount of cholesteryl palmitate incorporated into sphingomyelin (spectral features B and C in Fig. 3) remains unchanged at 1.5 mol% throughout the entire range of temperatures studied. Our results are in contrast with the conclusion reached by Janiak et al. [23] for a related system. They studied the cholesteryl myristate/dimyristoyl phosphatidylcholine/H_2O system using polarizing light microscopy, X-ray diffraction and differential scanning calorimetry and concluded that there was negligible incorporation of ester in the phospholipid below the phase transition temperature. The 1.5% incorporation of cholesteryl palmitate into sphingomyelin dispersions is approx. 8 times larger than the incorporation of cholesteryl palmitate into egg yolk phosphatidylcholine [4]. This increased solubility of ester in sphingomyelin membranes will make possible a study using cholesteryl palmitate selectively deuterated at various positions along the fatty acid chain, and such a study should give insight into the average conformation for the ester in the sphingomyelin membrane.

The widths of the powder patterns of the cholesteryl palmitate-d_{31} ^2H-NMR spectra in sphingomyelin (Fig. 2) and in egg phosphatidylcholine [4] aqueous dispersions are similar at equivalent temperatures above the phase transition, T_m, of the respective phospholipids. Also, from Figs. 2 and 4 we see that, at the higher temperatures, the slopes of the width vs. temperature plots for $(C^2H_2)_n$ and C^2H_3 decrease significantly, as observed for cholesteryl palmitate in egg phosphatidylcholine between 20 and 50° C. This suggests that, at equivalent temperatures well above T_m, the dynamic structure of the ester may be similar in different types of phospholipid.

The width of the ^2H-NMR signal for the $(C^2H_2)_n$ groups of cholesteryl palmitate-d_{31} varies by more than 2-fold between 40 and 55° C, whereas the width for $(C^2H_2)_n$ of dipalmitoyl phosphatidylcholine-d_{62} changes by less than one-half in the same temperature range (Fig. 2). A recent study [24] has demonstrated that the quadrupolar splitting from the acyl chain C-10 position in *N*-palmitoyl-10, 10-d_2-sphingomyelin in water shows the same behavior as dipalmitoyl phosphatidylcholine-d_{62}. This comparison indicates that the cholesteryl palmitate chains have quite different dynamic structural organization from the acyl chains of the phospholipids in which they dissolve.

A narrow isotropic signal, superimposed upon a lamellar phase powder pattern (Fig. 2), is characteristic of ^{31}P spectra for sphingomyelin dispersions [11,12]. The isotropic ^{31}P signal of sphingomyelin has been found to be absent at low water concentration [11] and to become of greater relative intensity at high water content [12], which may suggest that it arises from small bilayer structures for which rotational tumbling and lateral diffusion produce motional averaging. If this is the case, a crude estimate of the size of structures in the sphingomyelin/cholesteryl palmitate/water sample giving rise to the isotropic line may be made from the ^{31}P data. This estimation involves the calculation of an average correlation time, τ_c, for the isotropic sphingomyelin motion, using the following expression [25]:

$$\pi\Delta\nu_{1/2} = M_{2r}\tau_c \tag{6}$$

where $\Delta\nu_{1/2}$ = linewidth of the isotropic component, and M_{2r} ($= \frac{4}{45}\Delta\sigma_{eff}^2$) is the second moment of the lamellar phase powder pattern component (it is assumed that $M_{2r}\tau_c^2 << 1$ and a small τ_c-independent contribution to the linewidth is omitted). From the chemical shift anisotropy (in rad $\cdot$ s^{-1}) for multilamellar sphingomyelin, we calculate $M_{2r} \approx 1 \cdot 10^7 s^{-2}$. The corresponding correlation time $\tau_c \approx 50$ μs may be related to a weighted average radius, $\bar{R}$, of small spherical bilayer structures * tumbling freely in aqueous solution by [26]:

$$\tau_c^{-1} = \frac{6D}{\bar{R}^2} + \frac{3kT}{4\pi\bar{R}^3\eta} \tag{7}$$

where k is Boltzmann's constant, T is the absolute temperature, η is the viscosity of the medium and D is the lateral diffusion coefficient of the structure. Assuming a diffusion coefficient of $D \approx 10^{-8}$ cm^2 $\cdot$ s^{-1} for liquid crystalline phospholipid, an average radius $\bar{R} \approx 400$ Å is obtained. This radius is well below the minimum size ($\bar{R} \geqslant 1000$ Å) for which a low-field shoulder is still distinguished in the ^{31}P lamellar phase powder pattern at 40 MHz (Burnell, E.E., de Kruijff, B. and Cullis, P.R., unpublished results).

If we apply Eqn. 6 to our ^2H-NMR data using $M_{2r} \approx 8 \cdot 10^7 s^{-2}$ ($M_{2r} = \frac{1}{5}\Delta\omega^2$ where $\Delta\omega = 2\pi\Delta\nu_Q$) and $\Delta\nu_{1/2} \approx 400$ Hz, we find $\tau_c \approx 20$ μs for cholesteryl palmitate undergoing isotropic rotation in sphingomyelin. Considering the assumption inherent in these calculations and the difference in M_{2r} for the two measurements, the ester correlation time based on the ^2H-NMR data is consistent with that calculated from the ^{31}P-NMR data for the sphingomyelin. This suggests that the same motional processes are responsible for the narrow spectral component observed for ester and phospholipid, hence we propose that the ester giving rise to the isotropic ^2H-NMR signal is dissolved in that sphingomyelin undergoing isotropic reorientations. The similarity in the temperature dependence of the fraction of isotropic ^{31}P signals and of ^2H signals (Fig. 7) supports this interpretation.

---

* Clearly, the above is an oversimplification since it is highly unlikely that a single size of structure would be present and a distribution of sizes would result in a distribution of correlation times. Then the τ_c value we estimate from the linewidth of the isotropic line represents a weighted average over the distribution of sizes and the radius we calculate is smaller than the mean radius.

Addition of cholesterol to the sphingomyelin/cholesteryl palmitate aqueous dispersion decreases the solubility of cholesteryl palmitate in the phospholipid from 1.5 to less than 0.1 mol%. This decrease in ester solubility in phospholipid bilayers caused by cholesterol addition has been observed previously [27] in egg phosphatidylcholine unilamellar vesicles using ^{2}H-NMR spectroscopy and chemical analysis. Since the amount of cholesterol found in smooth muscle cell membranes in human aorta increases with progression of atherosclerosis [28], this may explain the low solubility of cholesteryl esters in this membrane. Cholesteryl esters coalesce in the interior of smooth muscle cells, the clinical manifestation of which is the so-called 'foam cell'.

References

1 Lang, P.D. and Insull, W. (1970) J. Clin. Invest. 49, 1479—1488
2 Pries, C. and Klynstra, F.B. (1971) Lancet, 750—751
3 Forrest, B.J. and Cushley, R.J. (1977) Atherosclerosis 28, 309—318
4 Valic, M.I., Gorrissen, H., Cushley, R.J. and Bloom, M. (1979) Biochemistry 18, 854—859
5 Böttcher, C.J.F. and van Gent, C.M. (1961) J. Atheroscler. Res. 1, 36—46
6 Seelig, J. (1977) Q. Rev. Biophys. 10, 353—418
7 Mantsch, H.H., Saito, H. and Smith, I.C.P. (1977) Prog. NMR Spectrosc. 11, 211—271
8 Davis, J.H., Jeffrey, K.R., Bloom, M., Valic, M.I. and Higgs, T.P. (1976) Chem. Phys. Lett. 42, 390—394
9 Seelig, J. (1978) Biochim. Biophys. Acta 515, 105—140
10 Yeagle, P.L., Hutton, W.C. and Martin, R.B. (1978) Biochemistry 17, 5745—5750
11 Cullis, P.R. and Hope, M.J., (1980) Biochim. Biophys. Acta, in the press
12 Cushley, R.J., Forrest, B.J., Grover, A.K. and Wassall, S.R. (1980) Can. J. Biochem. 58, 206—212
13 Grover, A.K. and Cushley, R.J. (1979) J. Labelled Compd. Radiopharmacol. 16, 307—313
14 Carter, H.E., Haines, W.J., Ledyard, W.E. and Norris, W.P. (1947) J. Biol. Chem. 169, 77—82
15 Sweeley, C.C. (1963) J. Lipid. Res. 4, 402—406
16 Calhoun, W.I. and Shipley, G.G. (1979) Biochim. Biophys. Acta 555, 436—441
17 Shipley, G.G., Avecilla, L.S. and Small, D.M. (1974) J. Lipid Res. 15, 124—131
18 Barenholz, Y., Suurkuusk, J., Mountcastle, D., Thompson, T.E. and Biltonen, R.L. (1976) Biochemistry 15, 2441—2447
19 Calhoun, W.I. and Shipley, G.G. (1979) Biochemistry 18, 1717—1722
20 Davis, J.H. (1979) Biophys. J. 27, 339—358
21 Burnett, J.L. and Müller, B.H. (1971) J. Chem. Phys. 55, 5829—5831
22 Davis, J.H. and Jeffrey, K.R. (1977) Chem. Phys. Lipids 20, 87—104
23 Janiak, M.J., Small, D.M. and Shipley, G.G. (1979) J. Lipid Res. 20, 183—199
24 Neuringer, L.J., Sears, B., Jungalwala, F.B. and Shriver, E.K. (1979) FEBS Lett. 104, 173—175
25 Abragam, A. (1961) The Principles of Nuclear Magnetism, 424-ff, Oxford University Press.
26 Bloom, M., Burnell, E.E., Valic, M.I. and Weeks, G. (1975) Chem. Phys. Lipids 14, 107—112, 363
27 Gorrissen, H., Tulloch, A.P. and Cushley, R.J. (1980) Biochemistry, in the press
28 Papahadjopoulos, D. (1974) J. Theor. Biol. 43, 329—337